Russian Journal of Earth Sciences, Vol. 22, ES01SI11
https://doi.org/10.2205/2022ES01SI11

Russian Journal of Earth Sciences

Special Issue: "Fundamental and Applied Aspects of Geology, Geophysics and Geoecology"

Atmospheric turbulence structure above urban nonhomogeneous surface

I. D. Drozd[1,2], I. A. Repina*[,1,2,3], A. V. Gavrikov[4], V. M. Stepanenko[1,2], A. Yu. Artamonov[2], A. D. Pashkin[2], and A. I. Varentsov[1,2]

[1]*Lomonosov Moscow State University, Geographic Faculty, Moscow, Russian Federation*
[2]*A. M. Obukhov Institute of Atmospheric Physics RAS, Moscow, Russia*
[3]*Maykop State Technology University, Maykop, Russia*
[4]*Shirshov Institute of Oceanology RAS, Moscow, Russia*

Received 1 July 2021; accepted 10 August 2022; published 3 November 2022.

A new 21-meter eddy covariance tower is installed in the Meteorological observatory of Moscow State University in November 2019. It includes 3 levels with METEK sonic anemometers. The mast is located inside the urban area and makes it possible to analyze the structure of atmospheric turbulence in a heterogeneous urban condition. The measurement data from November 2019 to May 2020 are processed. Turbulent fluctuations of the wind velocity components are found to increase with height within 20 meters above the surface. The turbulent kinetic energy is proportional to the square of the averaged horizontal wind speed. The drag coefficient is determined by the type of footprint surface, with a value of 0.08 and 0.05 for urbanized and vegetated surfaces, respectively. The "turbulent flux of heat flux" is reasonably well predicted by diagnostic relation with heat flux, skewness and standard deviation of vertical speed, suggesting significant contribution of coherent structures to turbulent fluxes. The daily amplitude of the temperature variance increases with the daily amplitude of the average temperature. The paper considers the conditions for the applicability of the Monin-Obukhov similarity theory to the calculation of turbulent fluxes over a heterogeneous urban landscape.

Keywords: atmospheric turbulence, urban climate, drag coefficient, Monin-Obukhov similarity theory, turbulent statistics, footprint.

Citation: Drozd, I. D., I. A. Repina, A. V. Gavrikov, V. M. Stepanenko, A. Yu. Artamonov, A. D. Pashkin, and A. I. Varentsov (2022), Atmospheric turbulence structure above urban nonhomogeneous surface, *Russian Journal of Earth Sciences*, Vol. 22, ES01SI11, doi: 10.2205/2022ES01SI11.

1 Introduction

Turbulent processes in the boundary layer of the atmosphere are the main mechanism for the exchange of energy and mass between the atmosphere and the surface. This exchange is governing on both short-term (synoptic) and climatic time scales. Therefore, a realistic mathematical description of turbulent processes at the surface is an important component of the successful solution of problems of atmospheric dynamics numerical prediction. However, the stochastic nature of turbulence crucially complicates the creation of a unified theory of turbulent exchange, so modern models use simplified schemes for calculating energy exchange with the surface, based on the Monin-Obukhov similarity theory (MOST), which assumes horizontal statistical uniformity of the underlying surface [*Monin and Obukhov*, 1954]. This simplification reduces the accuracy of the forecast, especially in regions with complex (heterogeneous) orography, such as in urban conditions.

Land surface heterogeneity is of different types and manifests itself over a wide range of spatial scales. Its multiscaling makes it nearly impossible to "resolve" all spatial information directly in geophysical modeling [*Giorgi and Avissar*, 1997] or in the analysis of observational data [see *Foken et al.*, 2010]. The scales of flow motions range from 1 mm (Kolmogorov microscale) to spatial scales of several kilometers or more. Thus, surface inhomogeneity is a problem that is practically impossible

*Corresponding author: repina@ifaran.ru

to solve taking into account all scales of interaction. But the problem of surface heterogeneity cannot be ignored or circumvented in the diagnosis and modeling of the atmospheric boundary layer (ABL) [*Pitman*, 2003; *Prueger et al.*, 2012]. Surface heterogeneity is a determining factor in the development of the atmospheric boundary layer under sea and urban breezes, in the dynamics of the boundary layer at the installation sites of wind power plants, in the formation of heat and evaporation fluxes over lakes and reservoirs, as well as in exchange processes over heterogeneous agricultural and urban areas or over ice covered sea with leads, melt ponds and hummocks. The problem of studying atmospheric processes over landscapes with different scales of heterogeneities, parameterization of such territories in weather and climate forecast models, are widely discussed in the world scientific literature [*Bou-Zeid et al.*, 2020]. But, despite the active development of this topic in recent decades, the problems of taking into account the influence of the surface in weather and climate modeling are far from being satisfactorily solved. Numerous studies have been devoted to the general problem of abrupt changes in surface properties (roughness, temperature, humidity) along an interface that is either perpendicular or parallel to the prevailing surface wind direction. These conditions lead to the formation of internal boundary layers or to the occurrence of secondary circulations (for example, a breeze between land and sea). Cases of other flow directions have been considered extremely rarely [*Raasch and Harbusch*, 2001; *Anderson*, 2020]. Over heterogeneous terrain, the formation of internal boundary layers [*Garratt*, 1990; *Medjnoun et al.*, 2018], role of advection [*Rao et al.*, 1974; *Fontan et al.*, 2013; *Higgins et al.*, 2013], intensity of secondary circulations [*Raasch and Harbusch*, 2001; *Fontan et al.*, 2013], influence of measurement errors [*Esau*, 2007; *Kenny et al.*, 2017] are studied. Parameterizations for weather and climate models are developed based on these approaches [*Bou-Zeid et al.*, 2004; *Ament and Simmer*, 2006; *Stoll and Porte-Agel*, 2009; *Li et al.*, 2013]. The interaction of several types of heterogeneity is even more complex, and the uniqueness of each heterogeneity model requires some simplified approaches to parameterize the combined effect of surface variability in regional and global atmospheric models.

Facing this complex frame, different approaches to the description of the atmospheric turbulence have been developed. From one hand, extensions of similarity have been proposed in order to take into account the presence of mesomotions, going beyond MOST by using different relations for specific cases [*Sun et al.*, 2012] or adding new parameters [*Stiperski et al.*, 2021]. In particular, assessing the applicability of the MOST theory in complex terrain and urban environments, identifying the departures of its formulations and investigating possible corrections, is since long an established field of research [*Mahrt*, 2010; *Mortarini et al.*, 2013; *Falabino and Trini Castelli*, 2017]. On the other hand, the equations for the ensemble averaged second order moments has been used as a frame to understand and model the behavior of stably stratified ABL. Different solutions of the higher momentum steady state and homogeneous equations result for different parameterizations of the third order moments (in particular, the terms containing the covariances between velocity or temperature and pressure) and of the dissipation.

Experimental data are needed to study the statistical characteristics of the turbulence of the atmospheric boundary layer in urban environment. The obtained regularities in the future may allow us to generalize the MOST for use in an inhomogeneous landscape. This paper presents the first results of the study of the mechanisms that cause the turbulent exchange over the geometrically complex surface of the city according to the micrometeorological mast installed in the Meteorological Observatory (MO) of Moscow State University (MSU).

2 Micrometeorological mast of the Moscow State University

In 2019, a 21-meter micrometeorological mast was put into operation on the territory of the MSU MO. There are both highly urbanized areas (the Belozersky Research Institute of the Russian Academy of Sciences, the MSU Greenhouse Building, the Ramenki district) and extensive areas of parks (the MSU Botanical Garden, the MSU Big Lawn, the Vorobyovy Gory nature reserve) in the immediate vicinity of the observatory (Figure 1a). Thus, the location of the mast allows to observe the formation of turbulent vortices and flows in different city landscapes depending on the wind direction, i.e. with the appropriate areas of influence ("footprint"), which makes it possible to study different modes of turbulence formation over an inhomogeneous underlying surface.

The micrometeorological mast is equipped with three measuring levels at altitudes of 2.2 m, 11.1 m and 18.8 m (Figure 1b). At each level, acoustic anemometers manufactured by METEK are installed, at the two lower levels – uSonic-3 Scientific (Figure 1c), at the upper – uSonic-3 class A. Vaisala's HMP155 humidity and temperature probe are additionally installed at the 2.2 m and 11.1 m levels. Acoustic anemometers with a frequency of 20 Hz record three components of wind

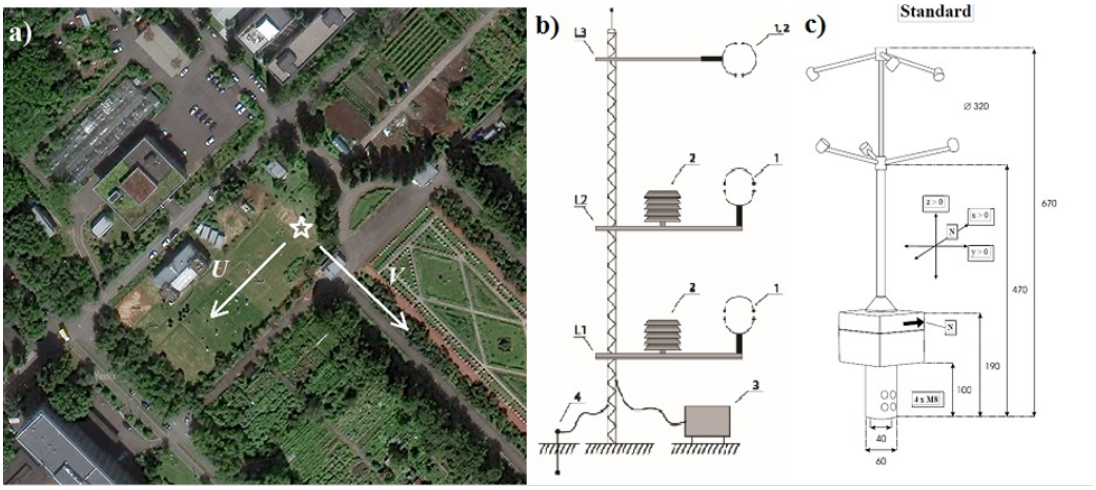

Figure 1: a) The location of the micrometeorological mast (marked with a star) and the direction of the axes of acoustic anemometers; b) The layout of the devices on the micrometeorological mast in the Moscow State University MO: measurement levels – L1, L2, L3; acoustic anemometers – 1; humidity and temperature sensors – 2; data collection unit – 3; ground loop – 4; c) The diagram of the uSonic-3 Scientific anemometer from the manufacturer's website (https://metek.de).

speed with an accuracy of 0.1 m/s and acoustic temperature with an accuracy of 0.1 °C. The axes of the instruments are oriented along Michurinskaya alley (speed component u) and on the Main Building of the MSU (speed component v) (Figure 1b). This article presents the result of the analysis of the data series obtained from the mast for the period from November 2019 to May 2020.

3 Data processing

The main experimental method for determining turbulent fluxes is the eddy covariance technique (EC). The essence of the method is to represent a rapidly changing quantity as the sum of the mean value and fluctuations ($T = \overline{T} + T'$) [*Reynolds*, 1895]. This representation allows to calculate fluxes as the covariance (i.e. averaged multiply fluctuations):

$$H = \overline{\rho_a} C_p \overline{w'T'},$$

$$\tau = \overline{\rho_a} \sqrt{\left(\overline{u'w'}\right)^2 + \left(\overline{v'w'}\right)^2},$$

where H is the sensible heat flux, τ is the absolute value of momentum flux, v', u', w' are the fluctuations of the velocity components, T' is the temperature fluctuations, ρ_a is the air density, the overbar denotes the mathematical expectation estimated as the mean value of the time series [*Burba*, 2013].

To implement the eddy covariance technique, the initial 20 Hz data from the anemometers are sorted by time to obtain a single chronological sequence. If the data contains gaps of less than one minute, they are filled with random values generated using a Gaussian distribution, the parameters of which are determined from the data before and after the gap. Gaps of more than one minute are not filled in. The filter block eliminates extremes that go beyond three-sigma limits, replacing them with the mathematical expectation of neighboring values. This methodology is widely used in the processing of turbulent measurements [*Aubinet et al.*, 2012].

A constant correction of +0.286 °C is introduced to the acoustic temperature data at the level of 11.1 m, it was set during the mutual calibration of the devices in the fall of 2019. Based on the obtained high-frequency data, statistical moments of the first and second order are calculated with averaging over 20-minute periods. The averaging period of 20 minutes makes it possible to clearly reproduce the diurnal variation of the turbulent characteristics, as well as to take into account the contribution of large-scale flow structures to the turbulent fluxes.

The processed measurement data for the example of March 2020 are presented in Figure 2.

Figure 2a and Figure 2b show how the horizontal wind speed increases with altitude. The maximum 20-minute average value of the horizontal speed modulus in March was recorded on March 13 at the level of 18.8 m and amounted to 6.5 m/s. Figure 2c indicates systematically positive values of the vertical speed at a height of 2.2 m, this fact raises doubts about the accuracy of the data obtained from this level and requires additional verification of the correctness of the lower anemometer. Figure 2d clearly shows the diurnal temperature variation, the minimum for March was −4 °C, and the maximum was recorded on March 28 (14 °C). The nights from March 14 to 15 and from

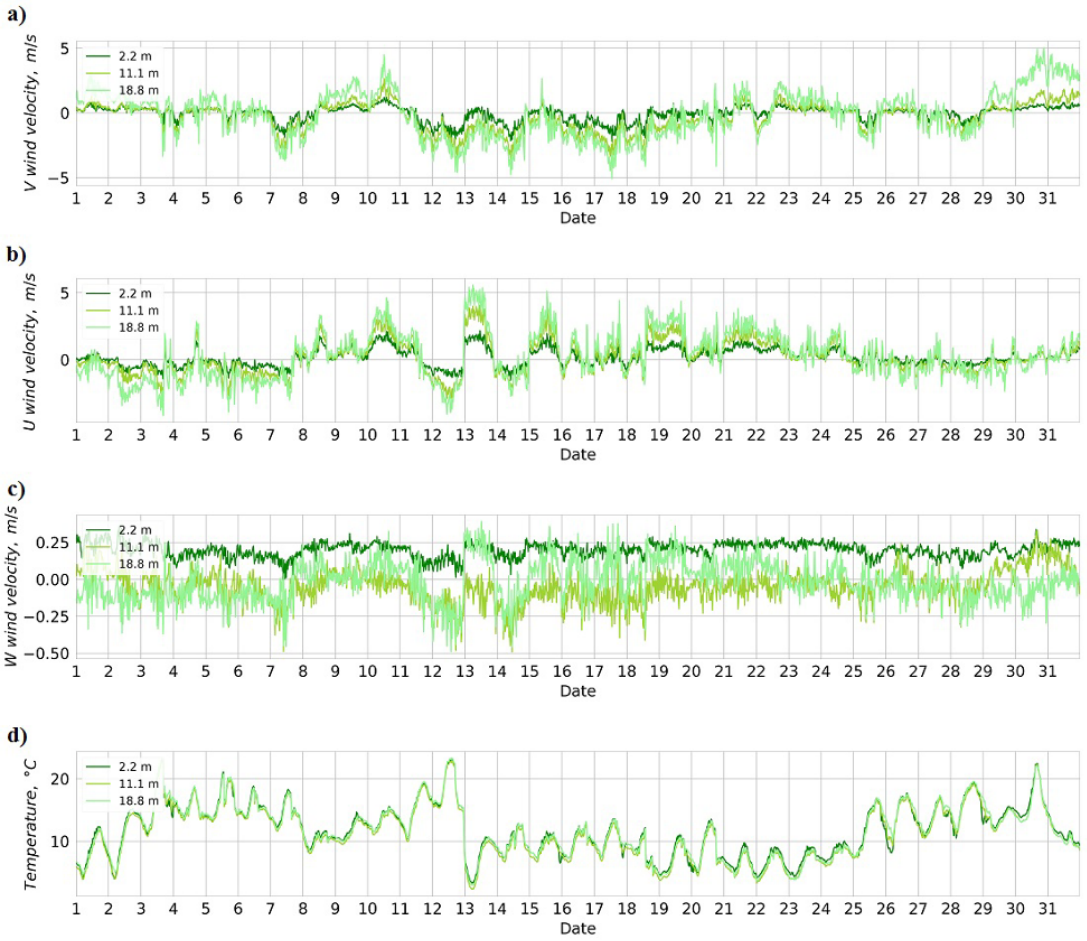

Figure 2: The characteristics measured on the micrometeorological mast in May 2020, averaged over 20-minute intervals: a) and b) horizontal components of wind speed; c) vertical wind speed; d) acoustic temperature. Line colors indicate measurement levels.

March 29 to 30 are characterized by a sharp drop in temperature by 15 °C, which, combined with increased wind speed on these dates, indicates the passage of a cold front.

The wind speed data series obtained from the micrometeorological mast on the example of November 2019 were compared with the data of the automatic meteorological complex of the MSU MO Vaisala MAWS-301, which registers temperature and wind speed at an altitude of 15 m (Figure 3).

As can be seen in Figure 3a and Figure 3b, the data agree closely with each other. However, if the Pearson correlation coefficient is 0.96 for the series of temperature averaged over 20 minutes (the AMS data is agree best with the anemometer at 2 m), then for the wind speed the same coefficient was only 0.55. Such a low indicator can be explained by the difference in the position of the sensors horizontally and in height, which in conditions of a significantly inhomogeneous surface (the presence of buildings, tall trees) can lead to a significant difference in the measurement data.

4 Statistical characteristics of turbulence

Figure 4 shows the daily variation of the sensible heat flux, typical for the summer (a) and winter (b) periods. It can be seen that both under conditions of stable and unstable stratification, there is no layer of constant fluxes. Under stable conditions, the formation of secondary circulations is possible, which leads to a significant difference in the characteristics of turbulence in the lower layer in comparison with the overlying layers. Under instability conditions, more intense turbulent mixing is observed in the upper layer. The presented example shows the need for a more detailed study of the statistical characteristics of turbulence at different measurement levels.

The following statistical characteristics of turbulence were calculated from the obtained data series: root mean square deviation (RMSD) for the three components of wind speed and acoustic temperature, modulus and direction of horizontal wind speed, sensible heat and momentum fluxes,

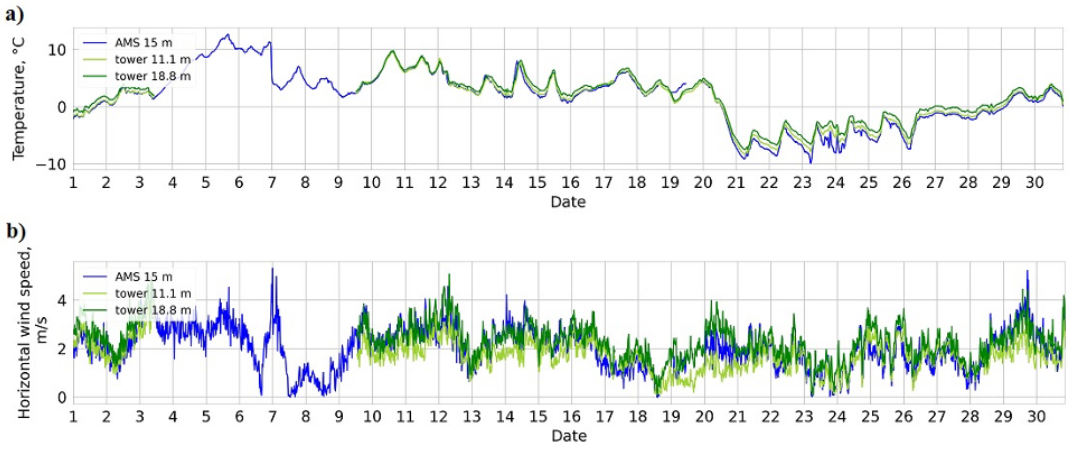

Figure 3: Comparison of the acoustic anemometer data averaged over 20 minutes with the data of the automatic meteorological station (AMS) for November 2019.

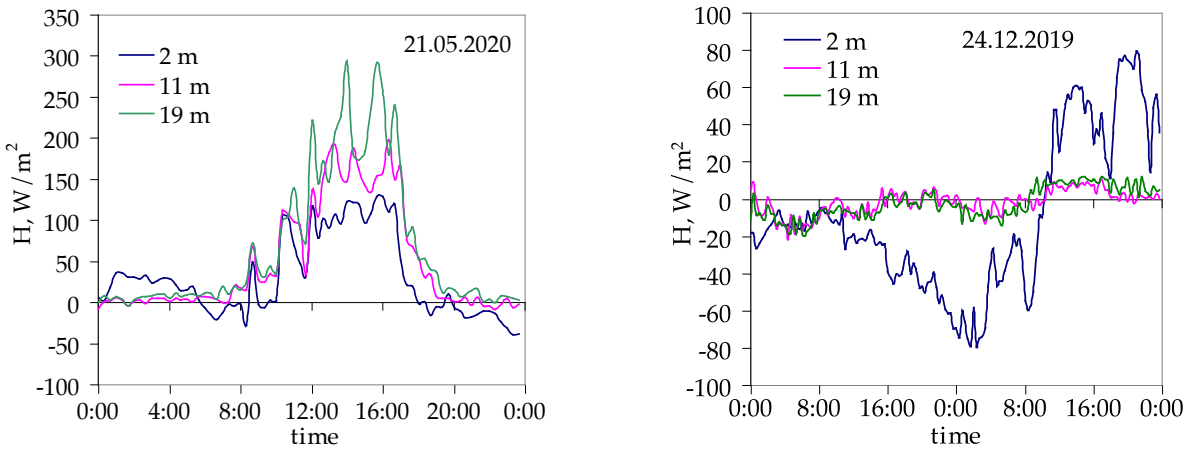

(a) summer **(b)** winter

Figure 4: Daily variation of sensible heat flux in summer and winter condition on the different measurement levels.

turbulent kinetic energy (TKE), and the proportion of vertical movements in the TKE. The main regularities of the behavior of the level of turbulence, determined by the values of the RMSD (dispersion) of the speed and temperature components, can be seen in Figure 5a.

An increase in RMSD with height is observed for all components of the wind speed; also, the TKE $K = \frac{1}{2}(\overline{u'}^2 + \overline{v'}^2 + \overline{w'}^2)$ increases with height. At the lower level, the speed dispersion approaches 0, since the speed identically turns to zero at the underlying surface. A similar result was obtained earlier from the measurements in a natural inhomogeneous landscape [*Barskov et al.*, 2019], as well as from large eddy simulation [*Glazunov and Stepanenko*, 2015]. Based on the data obtained, it can also be concluded that the intensity of turbulent pulsations in spring has a pronounced diurnal variation with a maximum in the daytime; this is due to an increase in both the wind speed and the instability of stratification in the daytime.

In this work, the correlation was also found between the daily amplitude of the temperature RMSD and the daily amplitude of the temperature (Figure 5b). Two hypotheses have been put forward about the reasons for this relationship. First – a large diurnal temperature amplitude may indicate a greater radiative heating of the underlying surface during the day, which increases turbulence due to the instability of the stratification. Thus, during the day, the amplitude of temperature pulsations becomes higher, and, accordingly, the difference in the amplitude of pulsations increases between day and night. Second – in an urban environment, the underlying surface is extremely inhomogeneous, at least because of the differences in albedo, greater radiation heating contributes to a greater contrast in the temperature of different surfaces. These contrasts are transmitted to the near-

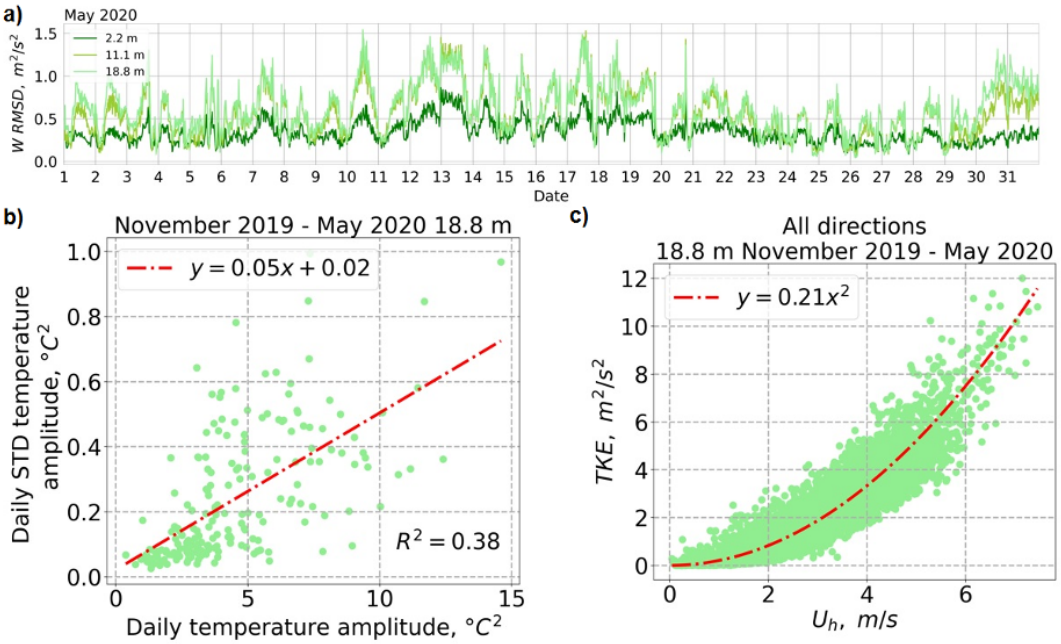

Figure 5: a) RMSD of vertical speed on the example of May 2020; b) the dependence of the daily amplitude of the 20-minute temperature RMSD on the daily amplitude of the average temperature for the period November 2019 – May 2020; c) the dependence of the turbulent kinetic energy on the horizontal wind speed modulus for the period November 2019 – May 2020.

surface air using thermal conductivity and then advected by an average flow from the generation region to the measurement point. To test these hypotheses, it is necessary to involve data from radiation measurements, this will be done in the subsequent stages of the work.

The relationship between the turbulent kinetic energy K and the horizontal speed modulus is well described by the quadratic form (Figure 5c). It is noteworthy that from month to month, the proportionality coefficient remains almost unchanged, varying from 0.15 to 0.30, which indicates the stable nature of this relationship. The established square-law is consistent with the similarity theory for a homogeneous surface [*Monin and Obukhov*, 1954] (but with a different value of the proportionality coefficient) and is confirmed by other measurements.

According to the theory of the surface layer [*Monin and Yaglom*, 1975], the momentum flux can be represented as:

$$\tau = \overline{\rho_a} C_d u^2,$$

that is, the momentum flux is proportional to the square of the speed modulus, while the drag coefficient C_d depends on the nature of the underlying surface over which the flux is formed. In this regard, the study area was divided into sectors in the wind direction with relatively uniform surfaces, for which the drag coefficient can be considered constant (Figure 6a). Further, sorting the measurement data by wind direction (Figure 6b), diagrams of momentum flux scattering relative to the horizontal speed modulus were constructed for each of the selected sectors (Figure 6c, Figure 6d).

The values of the drag coefficient calculated from empirical data for the sectors "Michurinskaya alley" and "Tall trees" (Figure 6c, Figure 6d) are 0.07 and 0.14, respectively. The difference in these coefficients is a numerical indicator of the high inhomogeneity of the underlying surface in the observation area, which directly affects the formcsation of turbulent fluxes.

One of fundamental questions regarding turbulent exchange between complex surface and the atmosphere is what is the contribution of organized turbulent structures in the total momentum, heat and mass fluxes in the surface layer. A new method for identification of coherent structures in the eddy-covariance time series has been applied in [*Barskov et al.*, 2019], basing on approach first introduced in theoretical studies of convective boundary layer [*Abdella and McFarlane*, 1997; *Zilitinkevich et al.*, 1999]. This approach utilizes the fact that under dominance of large-scale coherent structures contribution to fluxes, second and third statistical moments are linked by algebraic relation, e.g. for the "flux of heat flux" we have:

$$\overline{w'w'T'} = C\overline{w'T'}S_w\sqrt{\overline{w'^2}}, \quad (1)$$

where $C \sim 1$ is non-dimensional constant, and S_w is skewness of vertical velocity. From time series measured at mast in the period November 2019 – May 2020, we found that (1) indeed explains

much of third moment variability (Figure 7) with $C = 1.84$ at 11 m and $C = 1.39$ at 18 m. This suggests the significance of coherent structures for vertical flux formation over geometrically complex surface, which is agrees with estimates found earlier in natural [*Barskov et al.*, 2019] and urban landscapes [*Pashkin et al.*, 2019].

The most stable ratio between $\overline{w'w'T'}_{th}$ and $\overline{w'w'T'}$is observed in the "Tall trees" sector (Figure 7c, Figure 7d), where the airflow overcomes tall trees and contributes to the generation of large-scale coherent structures.

5 Conclusions

Based on measurements on the micrometeorological mast of the MSU MO from November 2019 to May 2020, the following regularities were confirmed, which were previously obtained for other inhomogeneous landscapes:

1. Turbulent perturbations of the wind velocity components in urban conditions within the first tens of meters increase with height. The turbulent kinetic energy is proportional to the square of the average horizontal wind speed.
2. The drag coefficient is determined by the type of surface over which the flux is formed, with a value of 0.07 and 0.14 for urbanized and greened surfaces in the vicinity of the MSU MO, respectively.
3. The "turbulent flux of heat flux" is reasonably well predicted by diagnostic relation with heat flux, skewness and standard deviation of vertical speed, suggesting significant contribution of coherent structures to turbulent fluxes.

In addition, a new result was obtained that needs to be verified on a larger data set: the daily amplitude of the temperature dispersion increases in proportion to the increase in the daily amplitude of the temperature itself.

Acknowledgements. The data of measurements by the automatic meteorological complex of the MSU MO were kindly provided by E. Yu. Zhdanova. The work was partially supported by the Ministry of Science and Higher Education of Russia Ministry of Science and Higher Education of Russia (Agreements 075-15-2021-574 and 075-15-2022-284). Statistical data processing was supported by the RSF grant 21-17-00249.

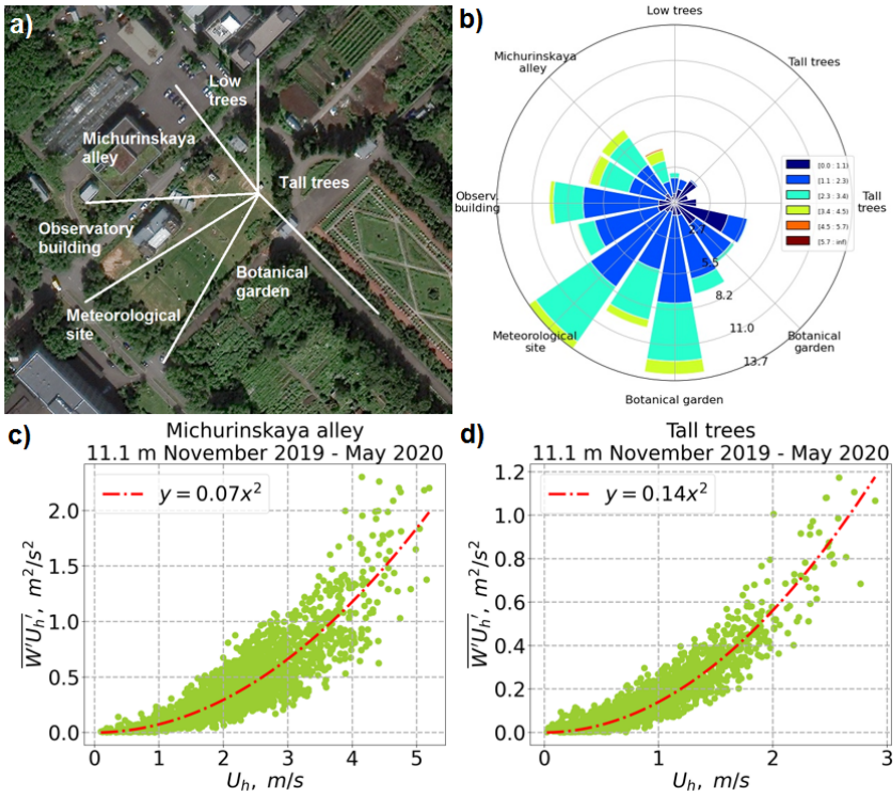

Figure 6: a) Division of the studied polygon into sectors by the direction of the wind; b) the wind rose according to data for the period November 2019 – May 2020 at 11.1 m; the dependence of the momentum flux on the horizontal speed modulus the period November 2019 – May 2020 for the sector "Michurinskaya alley" (c) and for the sector "Tall trees" (d).

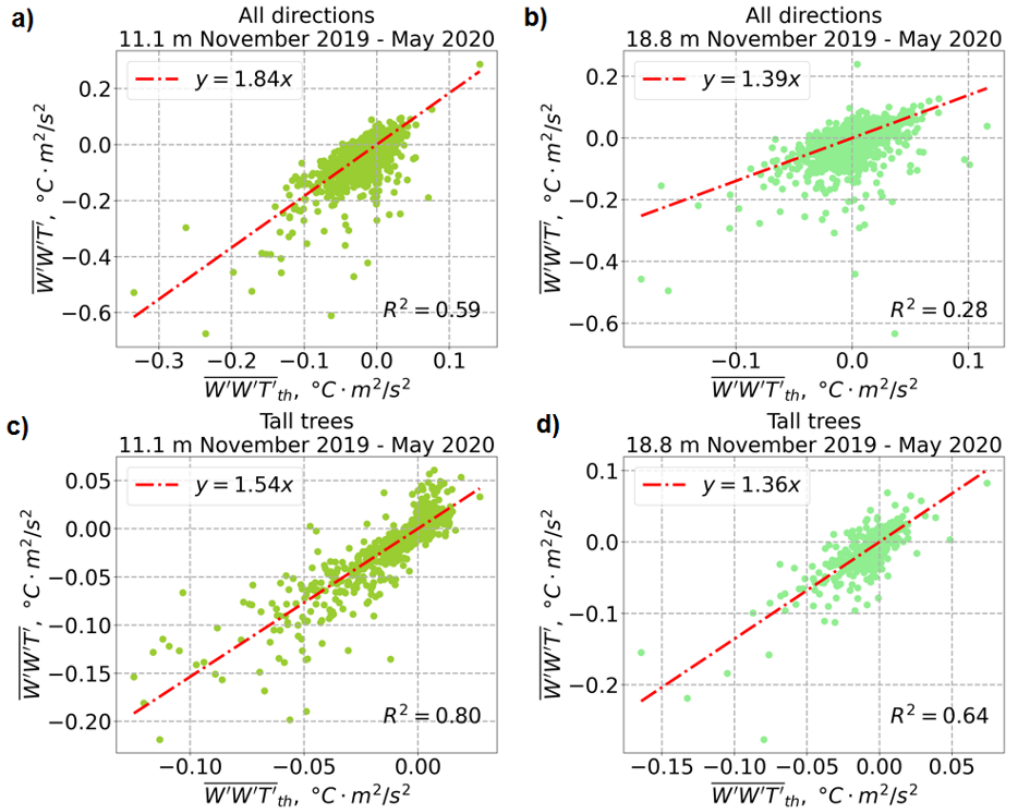

Figure 7: The scatter plot of theoretical $\overline{w'w'T'}_{th}$ computed according to (1), vs. measured $\overline{w'w'T'}$ in the period November 2019 – May 2020 for all wind directions (a),(b) and for the sector "Tall trees" (c), (d), at 11 m (left) and 18 m (right) height.

References

Abdella, K., and N. McFarlane, A New Second-Order Turbulence Closure Scheme for the Planetary Boundary Layer, *J. Atmos. Sci.*, *54*(14), 1850–1867, doi:10.1175/1520-0469(1997)054<1850:ANSOTC>2.0.CO;2, 1997.

Ament, F., and C. Simmer, Improved Representation of Land-surface Heterogeneity in a Non-hydrostatic Numerical Weather Prediction Model, *Boundary-Layer Meteorology*, *121*(1), 153–174, doi:10.1007/s10546-006-9066-4, 2006.

Anderson, W., Turbulent channel flow over heterogeneous roughness at oblique angles, *J. Fluid Mech.*, *886*, A15-1–A15-15, doi:10.1017/jfm.2019.1022, 2020.

Aubinet, M., T. Vesala, and D. Papale, *Eddy covariance: a practical guide to measurement and data analysis*, 442 pp., Dordrecht: Springer, doi:10.1007/978-94-007-2351-1, 2012.

Barskov, K. V., V. M. Stepanenko, I. A. Repina, A. Y. Artamonov, and A. V. Gavrikov, Two regimes of turbulent fluxes above frozen small lake surrounded by forest, *Bound.-Layer Meteorol.*, *173*(3), 311–320, doi:10.1007/s10546-019-00469-w, 2019.

Bou-Zeid, E., C. Meneveau, and M. B. Parlange, Large-eddy simulation of neutral atmospheric boundary layer flow over heterogeneous surfaces: Blending height and effective surface roughness, *Water Resources Research*, *40*(2), W02505, doi:10.1029/2003WR002475, 2004.

Bou-Zeid, E., W. Anderson, G. G. Katul, and L. Mahrt, The persistent challenge of surface heterogeneity in boundary-layer meteorology: a review, *Bound.-Layer Meteorol.*, *177*(2), 227–245, doi:10.1007/s10546-020-00551-8, 2020.

Burba, G., *Eddy Covariance Method for Scientific, Industrial, Agricultural and Regulatory Applications: a Field Book on Measuring Ecosystem Gas Exchange and Areal Emission Rates*, 331 pp., LI-COR Biosciences: Lincoln, USA, 2013.

Esau, I. N., Amplification of turbulent exchange over wide arctic leads: large-eddy simulation study, *J. Geophys. Res.*, *112*(D8), D08,109, doi:10.1029/2006JD007225, 2007.

Falabino, S., and S. Trini Castelli, Estimating wind velocity standard deviation values in the inertial sublayer from observations in the roughness sublayer, *Meteorology and Atmospheric Physics*, *129*(1), 83–98, doi:10.1007/s00703-016-0457-x, 2017.

Foken, T., M. Mauder, C. Liebethal, F. Wimmer, F. Beyrich, J.-P. Leps, S. Raasch, H. A. R. DeBruin,

W. M. L. Meijninger, and J. Bange, Energy balance closure for the LITFASS-2003 experiment, *Theoretical and Applied Climatology*, *101*(1), 149–160, doi:10.1007/s00704-009-0216-8, 2010.

Fontan, S., G. Katul, D. Poggi, C. Manes, and L. Ridolfi, Flume experiments on turbulent flows across gaps of permeable and impermeable boundaries, *Bound.-Layer Meteorol.*, *147*(1), 21–39, doi:10.1007/s10546-012-9772-z, 2013.

Garratt, J. R., The internal boundary layer – A review, *Bound.-Layer Meteorol.*, *50*(1), 171–203, doi:10.1007/BF00120524, 1990.

Giorgi, F., and R. Avissar, Representation of heterogeneity effects in earth system modeling: Experience from land surface modeling, *Reviews of Geophysics*, *35*(4), 413–437, doi:10.1029/97RG01754, 1997.

Glazunov, A. V., and V. M. Stepanenko, Large-eddy simulation of stratified turbulent flows over heterogeneous landscapes, *Izv. Atmos. Ocean Phys.*, *51*(4), 351–361, doi:10.1134/S0001433815040027, 2015.

Higgins, C. W., E. Pardyjak, M. Froidevaux, V. Simeonov, and M. B. Parlange, Measured and estimated water vapor advection in the atmospheric surface layer, *J. Hydrometeorol.*, *14*(6), 1966–1972, doi:10.1175/JHM-D-12-0166.1, 2013.

Kenny, W. T., G. Bohrer, T. H. Morin, C. S. Vogel, A. M. Matheny, and A. R. Desai, A Numerical Case Study of the Implications of Secondary Circulations to the Interpretation of Eddy-Covariance Measurements Over Small Lakes, *Bound.-Layer Meteorol.*, *165*(22), 311–332, doi:10.1007/s10546-017-0268-8, 2017.

Li, D., E. Bou-Zeid, M. Barlage, F. Chen, and J. A. Smith, Development and evaluation of a mosaic approach in the WRF-Noah framework, *J. Geophys. Res. Atmos.*, *118*(21), 11,918–11,935, doi:10.1002/2013JD020657, 2013.

Mahrt, L., Variability and maintenance of turbulence in the very stable boundary layer, *Bound.-Layer Meteorol.*, *135*(1), 1–18, doi:10.1007/s10546-009-9463-6, 2010.

Medjnoun, T., C. Vanderwel, and B. Ganapathisubramani, Characteristics of turbulent boundary layers over smooth surfaces with spanwise heterogeneities, *J. Fluid Mech.*, *838*, 516–543, doi:10.1017/jfm.2017.849, 2018.

Monin, A. S., and A. M. Obukhov, Basic laws of turbulent mixing in the surface layer of the atmosphere, *Contrib. Geophys. Inst. Acad. Sci. USSR*, *151*(24), 163–187, (In Russian), 1954.

Monin, A. S., and A. M. Yaglom, *Statistical Fluid Mechanics: Mechanics of Turbulence*, vol. 1, 874 pp., London Cambridge Mass.: MIT Press, 1975.

Mortarini, L., E. Ferrero, S. Falabino, S. Trini Castelli, R. Richiardone, and D. Anfossi, Low-frequency processes and turbulence structure in a perturbed boundary layer, *Quarterly Journal of the Royal Meteorological Society*, *139*(673), 1059–1072, doi:10.1002/qj.2015, 2013.

Pashkin, A. D., I. A. Repina, V. M. Stepanenko, V. Y. Bogomolov, S. V. Smirnov, and A. E. Telminov, An experimental study of atmospheric turbulence characteristics in an urban canyon, *IOP Conference Series: Earth and Environmental Science*, *386*, 012035, doi:10.1088/1755-1315/386/1/012035, 2019.

Pitman, A., The evolution of, and revolution in, land surface schemes designed for climate models, *Int. J. Climatol.*, *23*(5), 479–510, doi:10.1002/joc.893, 2003.

Prueger, J., J. Alfieri, L. Hipps, W. Kustas, J. Chavez, S. Evett, M. Anderson, A. French, C. Neale, L. McKee, J. Hatfield, T. Howell, and N. Agam, Patch scale turbulence over dryland and irrigated surfaces in a semi-arid landscape under advective conditions during BEAREX08, *Adv. Water. Resour.*, *50*, 106–119, doi:10.1016/j.advwatres.2012.07.014, 2012.

Raasch, S., and G. Harbusch, An analysis of secondary circulations and their effects caused by small-scale surface inhomogeneities using large-eddy simulation, *Bound.-Layer Meteorol.*, *101*(1), 31–59, doi:10.1023/A:1019297504109, 2001.

Rao, K. S., J. C. Wyngaard, and O. R. Cote, The structure of the two-dimensional internal boundary layer over a sudden change of surface roughness, *J. Atmos. Sci.*, *31*(3), 738–746, doi:10.1175/1520-0469(1974)031<0738:TSOTTD>2.0.CO;2, 1974.

Reynolds, O., On the dynamical theory of incompressible viscous fluids and the determination of the criterion, *Philosophical Transactions of the Royal Society of London, A*, *186*, 123–164, 1895.

Stiperski, I., M. Chamecki, and M. Calaf, Anisotropy of unstably stratified near-surface turbulence, *Bound.-Layer Meteorol.*, *180*(3), 363–384, doi:10.1007/s10546-021-00634-0, 2021.

Stoll, R., and F. Porte-Agel, Surface heterogeneity effects on regional-scale fluxes in stable boundary layers: surface temperature transitions, *J. Atmos. Sci.*, *66*(2), 412–431, doi:10.1175/2008JAS2668.1, 2009.

Sun, J., L. Mahrt, R. M. Banta, and Y. L. Pichugina, Turbulence regimes and turbulence intermittency in the stable boundary layer during cases-99, *J. Atmos. Sci.*, *69*(1), 338–351, doi:10.1175/JAS-D-11-082.1, 2012.

Zilitinkevich, S. S., V. M. Gryanik, V. N. Lykossov, and D. V. Mironov, Third-Order Transport and Nonlocal Turbulence Closures for Convective Boundary Layers, *J. Atmos. Sci.*, *56*(19), 3463–3477, doi:10.1175/1520-0469(1999)056<3463:TOTANT>2.0.CO;2, 1999.